AIP Conference Proceedings

Unifying framework for decomposition models of parametric and non-parametric image registration

Cite as: AIP Conference Proceedings **1870**, 050007 (2017); https://doi.org/10.1063/1.4995917
Published Online: 07 August 2017

Mazlinda Ibrahim, and Ke Chen

Unifying Framework for Decomposition Models of Parametric and Non-parametric Image Registration

Mazlinda Ibrahim[1, a)] and Ke Chen[2, b)]

[1]*Department of Mathematics, Centre for Defence Foundation Studies, National Defence University of Malaysia, Kem Sungai Besi, 57000 Kuala Lumpur, Malaysia.*
[2]*Centre for Mathematical Imaging Techniques and Department of Mathematical Sciences, The University of Liverpool, Liverpool, L69 7ZL, United Kingdom.*

[a)]Corresponding author: mazlinda@upnm.edu.my
[b)]K.Chen@liv.ac.uk

Abstract. Image registration aims to find spatial transformations such that the so-called given template image becomes similar in some sense to the reference image. Methods in image registration can be divided into two classes (parametric or non-parametric) based on the degree of freedom of the given method. In parametric image registration, the transformation is governed by a finite set of image features or by expanding the transformation in terms of basis functions. Meanwhile, in non-parametric image registration, the problem is modelled as a functional minimisation problem via the calculus of variations. In this paper, we provide a unifying framework for decomposition models for image registration which combine parametric and non-parametric models. Several variants of the models are presented with focus on the affine, diffusion and linear curvature models. An effective numerical solver is provided for the models as well as experimental results to show the effectiveness, robustness and accuracy of the models. The decomposition model of affine and linear curvature outperforms the competing models based on tested images.

INTRODUCTION

Image registration is an important area in imaging science, having broad applications such as target tracking, motion estimation, pattern recognition, satellite imagery and medical diagnosis. In medical image analysis, image registration is one of the crucial steps required to facilitate automatic feature extraction, treatment planning and other applications involving imaging machinery. Image registration is used to correct artifacts caused by the patient's movement as well as by disease progression, by aligning corresponding features between images. For a survey of image registration techniques, see [1,2,3,4,5,6] for more details.

There exist many image registration methods, but only few methods can meet the practical demand of a universally useful registration method: efficiency, robustness and accuracy. Here we follow the classification method in [5]:dividing registration models into either parametric or non-parametric categories based on the nature of geometric transformation (in terms of parameters). The first category of methods is parametric image registration, in which the transformation is governed by a finite set of image features or by expanding the transformation in terms of basis functions. One of the most commonly applied models in clinical applications is still affine (which has 6 parameters

Proceedings of the 24th National Symposium on Mathematical Sciences
AIP Conf. Proc. 1870, 050007-1–050007-11; doi: 10.1063/1.4995917
Published by AIP Publishing. 978-0-7354-1550-8/$30.00

[7]) because the automated solution has been proven to be accurate and has reached a degree of maturity in comparison with non-rigid image registration [4]. For more sophisticated parametric transforms such as cubic B-splines [8], the number of parameters can be larger e.g. 64 parameters. Nevertheless, a nonlinear least squares system with fewer than 1000 unknowns is not a computational challenge; consequently, all parametric registration methods are efficient, though registration accuracy depends on the input images. The second method is non-parametric which originates from modelling the transformation as physical displacement, so ideas of physical processes such as diffusion [9], elastic deformation [10] and curvature motion [11] are used for this class of registration.

In real life applications involving image registration, the spatial transformation to be recovered consists of large linear and non-linear displacement fields. The transformation can also be divided into global and local deformation. According to [12, 13], the linear and non-linear parts of a transformation can be represented by coarse and fine deformation, respectively. Therefore, one requires a registration scheme that can handle both (linear and nonlinear) and (global and local) deformation. One of the solutions to the above problem is to use non-parametric image registration models which are invariant to the linear transformation, such as linear curvature model by [11, 14], mean [15, 16] or Gaussian curvature models [17]. However, when one uses such methods, the global (linear) part of the transformation is only recovered using a large regularisation parameter which results in less fitting. To recover both (global-local and linear-non-linear) parts, we have to use a smaller level of regularisation. Thus, the quality of the recovered transformation is highly dependent on regularisation parameters. We present a unified framework for registration scheme called the decomposition models which are capable to handle cases with linear-nonlinear and global-local deformation. Second order regularisation based models such as the linear, mean and Gaussian curvature models will also benefit from this unifying framework. If we use the second order regularisation based models, there is no clear separation between the global and local (or linear and non-linear) parts of the transformation. With the decomposition model, the transformation is divided into two parts, thus we have a clear division between these two parts which allows for further processing tasks to both parts separately.

In this paper, we propose a decomposition model combining both parametric, for which we choose the affine linear model, and non-parametric transformations which possess the advantages of the two categories. In terms of effectiveness and accurate registration, first, alignment is carried out by the parametric part of the transformation and, second, alignment or deformation is modelled by the non-parametric part of the transformation. In terms of efficiency, the new model benefits from fast implementation of the parametric part of the transformation and also from a good initial guess to accelerate the solution of the non-parametric part of the transformation. We shall choose one affine based model for parametric transformation and the diffusion and linear curvature models for non-parametric transformations. The decomposition model is a general framework and other combinations are possible and may be studied later. However, from our numerical results, the decomposition model of affine and linear curvature turns to be the best combination based on the tested images.

RELATED WORK ON DECOMPOSITION MODELS

In this secton, we provide a brief review of mathematical formulation for image registration before reviewing several works on this task.

Denote the reference and template images, respectively as given functions of compact support $R, T : \Re^2 \to V \subset \Re^+$. The image domain is taken as $\Omega = [0,1]^2$. Here we focus on mono-modality images and V denotes the the range of intensities values; usually $V = [0,255]$. Let $\varphi = \varphi(\mathbf{x}) : \Omega \to \Re^2$ the unknown transformation aiming for $T(\varphi(\mathbf{x})) = R$ where $\mathbf{x} = (x_1, x_2)$. For non-parametric image registration, the transformation is written as $\varphi(\mathbf{x}) = \mathbf{x} + \mathbf{u}(\mathbf{x})$ to enable us to focus on the unknown displacement vector $\mathbf{u}(\mathbf{x})$. To obtain a unique solution to the registration problem, we solve

$$\min_{\mathbf{u}(\mathbf{x})} \{J(\mathbf{u}(\mathbf{x})) = D^{SSD}(\mathbf{u}(\mathbf{x})) + \gamma S(\mathbf{u}(\mathbf{x}))\} \qquad (1)$$

where D^{SSD} is a similarity measure, S is a regularisation term and λ is the regularisation parameter.

Coarse and Fine Registration

Here Modersitzki and Haber in [12, 13], proposed a combination of coarse and fine dimensional space of parametric and non-parametric image registration respectively. The coarse part of the transformation will handle the linear deformation and the non-linear part of the deformation is taken care by the fine part separately. The coarse and fine spaces are disjoint where the fine space is the remaining orthogonal complement of the coarse space. The authors consider affine linear transformation as the coarse part and linear elasticity model [10, 19, 20, 5] as the fine part. The total displacement field can be written as

$$\mathbf{u}(\mathbf{x}) = \mathbf{u}_{affine}(\mathbf{x}) + \mathbf{u}_{elastic}(\mathbf{x}) \qquad (2)$$

where $\mathbf{u}_{affine}(\mathbf{x})$ is based on affine linear model and $\mathbf{u}_{elastic}(\mathbf{x})$ is based on linear elastic non-parametric model. The model is given by

$$\min_{\mathbf{u}_{affine}, u_{elastic}} J^{COFIR} = D^{SSD}(T, R, \mathbf{u}_{affine}(x) + \mathbf{u}_{elastic}(x)) + \gamma S^{elastic}(\mathbf{u}_{elastic}(x)) \qquad (3)$$

The regularisation term for the linear elastic model is given by

$$S^{elastic}(\mathbf{u}) = \int_{\Omega} \frac{\mu}{4} \sum_{l,m=1}^{2} (\partial_{x_l} u_m + \partial_{x_m} u_l)^2 + \frac{\lambda}{4} (\text{ div } \mathbf{u})^2 \, d\Omega$$

where μ and λ are Lame constant. μ is the shear modulus that refers to the rigidity that estimates the stiffness of material and λ is related to the bulk modulus. The orthogonal complement of the fine part is embedded in the mode through incorporation of the following constraint

$$\mathbf{W}^T(\mathbf{x})\mathbf{u}_{elastic}(\mathbf{x}) = \mathbf{0}$$

where $\mathbf{W}$ is the basis function for the affine model.

Cubic B-spline and Total Variation Model

Hu et al. proposed in their 2014 paper [21], the combination of the parametric model based cubic B-spline and the non-parametric total variation model. The model in [21] is given by

$$\min_{\mathbf{u}(\mathbf{x})} J^{CBTV} = D^{RC}(T, R, \mathbf{u}(\mathbf{x})) + \gamma_1 S^{TV}(\mathbf{u}(\mathbf{x})) + \gamma_2 \left\| \mathbf{u}(\mathbf{x}) - \mathbf{u}^*_{cubicB-spline}(\mathbf{x}) \right\|_2^2 \qquad (4)$$

where $\gamma_i, i=1,2$ are the positive constant parameters. The distance measure for the mode is the residual complexity (RC) similarity measure proposed by Myronenko and Song in [22]. It is given by

$$D^{RC}(T,R,\mathbf{u}) = \log(\frac{\left\|Q^T(R-T(\mathbf{x}+\mathbf{u}(\mathbf{x}))\right\|^2}{\eta}+1)$$

where Q^T is the discrete cosine transform (DCT) basis and η is a trade-off parameter to measure the correlation of the noise in the template image. The regularisation in equation (2) is given by

$$S^{TV}(u(x)) = \int_\Omega \left|\nabla u_1(\mathbf{x})\right| + \left|\nabla u_2(\mathbf{x})\right| d\Omega$$

where $\left|\nabla u_l\right| = \sqrt{\left|\nabla u_l\right| + 1}, l = 1,2.$

A UNIFYING FRAMEWORK FOR DECOMPOSITION MODELS

Following the work by Modersitzki and Haber [12, 13] and Hu et al. [21], we consider generalising specific decomposition models to a framework which consists of any parametric and non-parametric models. Then we recommend and test on two particular choices. Starting from equation (1), we can write

$$\mathbf{u}(\mathbf{x}) = \mathbf{u}_{par}(\mathbf{x}) + \mathbf{u}_{non-par}(\mathbf{x}) \qquad (5)$$

where $\mathbf{u}_{par}(\mathbf{x})$ and $\mathbf{u}_{non-par}(\mathbf{x})$ are the displacement fields from parametric and on-parametric models respectively. Two variants of the model in equation (3) are

$$\text{Model A}: \mathbf{u}(\mathbf{x}) = \mathbf{u}_{affine}(\mathbf{x}) + \mathbf{u}_{diff}(\mathbf{x}) \qquad (6)$$

$$\text{Model B}: \mathbf{u}(\mathbf{x}) = \mathbf{u}_{affine}(\mathbf{x}) + \mathbf{u}_{LC}(\mathbf{x}) \qquad (7)$$

to be included in numerical tests in Section 4. The diffusion and linear curvature (LC) regularisation terms for non-parametric image registration models are given by

$$S^{diff}(\mathbf{u}(\mathbf{x})) = \int_\Omega \left|\nabla u_1\right|^2 + \left|\nabla u_2\right|^2 d\Omega \qquad (8)$$

and

$$S^{LC}(\mathbf{u}(\mathbf{x})) = \int_\Omega (\Delta u_1)^2 + (\Delta u_1)^2 d\Omega \qquad (9)$$

respectively. Others variants of the decomposition models are

$$\text{Model} \quad C: \mathbf{u}(\mathbf{x}) = \mathbf{u}_{cubic\ B-spline}(\mathbf{x}) + \mathbf{u}_{diff}(\mathbf{x}) \qquad (10)$$

$$\text{Model} \quad D: \mathbf{u}(\mathbf{x}) = \mathbf{u}_{cubic\ B-spline}(\mathbf{x}) + \mathbf{u}_{LC}(\mathbf{x}) \qquad (11)$$

where $\mathbf{u}_{cubic\ B-spline}(\mathbf{x})$ is as in [8,23]. The model in equation (5) is not limited to (6), (7), (10) , and (11) but easily extended to any parametric and non-parametric models. We can write the decomposition model using (5) as

$$\min_{\mathbf{u}_{par}(\mathbf{x}),\mathbf{u}_{non-par}(\mathbf{x})} J^{Decompose} = D^{ssd}(T, R, \mathbf{u}_{par}(\mathbf{x}) + \mathbf{u}_{non-par}(\mathbf{x})) + \gamma S(\mathbf{u}_{non-par}(\mathbf{x})) \qquad (12)$$

subject to

$$K\mathbf{u}_{non-par}(\mathbf{x}) = \mathbf{0}$$

where K is the basis function for the parametric model. For example, $K = \mathbf{W}^T$ for the affine model. As in [12, 13], the constraint is a vital aspect in the decomposition model because the term guaranteed that the non-parametric part of the transformation is in the remaining orthogonal complement of the space of parametric transformation. We use the following Lagrangian term to incorporate the constraint

$$L(\mathbf{u}_{par}(\mathbf{x}), \mathbf{u}_{non-par}(\mathbf{x}), \mathbf{p}) = D^{ssd}(T, R, \mathbf{u}_{par}(\mathbf{x}) + \mathbf{u}_{non-par}(\mathbf{x})) + \lambda S(\mathbf{u}_{non-par}(\mathbf{x})) + \mathbf{p}^T W^T \mathbf{u}_{non-par}(\mathbf{x})$$

where $\mathbf{p}^T$ is the Lagrange multipliers. For the affine model we have

$$\mathbf{p}^T = [p_1, p_2, p_3, p_4, p_5, p_6]^T$$

The functional in (12) uses the sum of squared difference as the distance measure to quantify the differences between the transformed template and reference images which is optimal for mono-modal image registration with Gaussian noise. It can be easily extended for more sophisticated distance measures such as the residual complexity and mutual information for multi-modality image registration.

We use the standard coarsening and full-weighting restriction operator in multigrid [24] applications to obtain the coarse representation of the template and reference images. For the interpolation operator, we use the bilinear interpolation which is the adjoint operator to the full-weighting restriction operator. However, as in [12, 13], special treatment is added in the interpolation operator to $\mathbf{u}_{non-par}$ for maintaining the constraints. We would recommend Model B as in (7) because non-parametric model based on linear curvature will produce higher smoothness of the deformation field compared to the diffusion model as seen later in Section 4.

NUMERICAL RESULTS

We use one numerical experiment to examine the efficiency and robustness of Model A and B. For clarity we summarise the different models to be tested in Table 1. To judge the quality of the alignment we calculate the relative reduction of the similarity measure

$$\varepsilon = \frac{D^{ssd}(T, R, \mathbf{u})}{D^{ssd}(T, R)}$$

and the minimum value of the Jacobian matrix j of the transformation, denoted by F

$$j = \begin{bmatrix} 1+u_{1,x_1} & u_{1,x_2} \\ u_{2,x_1} & 1+u_{2,x_2} \end{bmatrix}, F = \min(\det(j))$$

We can observe that when $F > 0$, the deformed grid is free from folding and cracking. All experiments were run on multilevel.

TABLE 1. Description of the notation use to represent different models for comparison in Section 4.

Model	Description
COFIR	Model (3) which is the coarse and fine image registration by [12,13].
CBTV	Model (4) which is using Cubic B-spline and total variation model by Hu et. al [21] .
M1A	Diffusion image registration model using (1) and (8) .
M1B	Linear curvature image registration model using (1) and (9).
M2A	Diffusion image registration with affine as pre-registration.
M2B	Linear curvature image registration with affine as pre-registration.
M3A	Our new Model A using affine and diffusion .
M3B	Our new Model B using affine and linear curvature.

Test 1: Real Images

Images for Test 1 are taken from [6] where X-ray images of two hands of different individuals need to be aligned. The size of the images is 128 x128 and they consist of global rotation and translation and also local deformations. The reference, template images and the difference before registration are shown in Figure 1.

(a) (b) (c)

FIGURE 1. Test 1: from left to right. (a) is the reference image, (b) is the template image and (c) is the difference between the reference and template images before registration.

The results for the diffusion model with three different approaches including Model A are shown in Figure 2. The diffusion model alone is not able to solve this particular problem since the model is variant to the affine model as shown in Figures 2 (a) and (d). The model is stuck at the local minima, thus we obtain large value of $\varepsilon = 0.2346$. The lowest value of ε is given by M3A in Figures 2 (c) and (f) where $\varepsilon = 0.0557$.

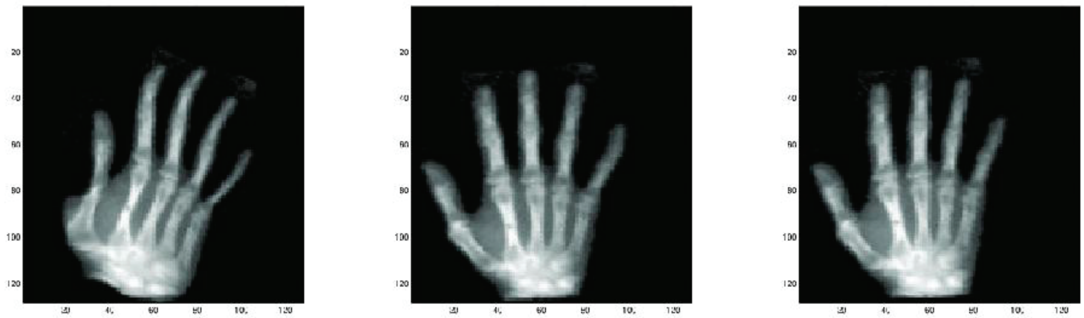

(a) M1A, $\varepsilon = 0.2346$ (b) M2A, $\varepsilon = 0.1328$ (c) M3A, $\varepsilon = 0.0557$

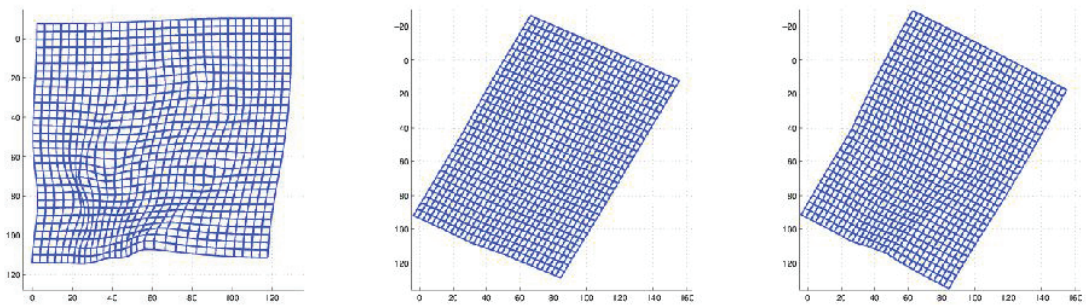

(d) $\gamma = 0.09, F = 0.0430$ (e) $\gamma = 0.5, F = 0.7575$ (f) $\gamma = 0.1, F = 0.5955$

FIGURE 2. Test 1: from left to right and top to bottom. Top row: (a) is the transformed template images using the diffusion image registration method. (b) is the resulting transformed template image using the diffusion and affine as a pre-registration. (c) is the transformed template image using the decomposition model with affine and diffusion models. The images on the bottom row are the corresponding deformations to the top row applied on regular grid. We can observe that the lowest value of ε is given by the decomposition model indicates higher similarity between the reference and the transformed template images.

The results for the linear curvature model including Model B (M3B) for Test 1 are shown in Figure 3. In Figure 3 linear curvature is able to solve this problem since it is a second order regularisation based model. The results also confirm that the linear curvature in particular and the second order terms in general are better than diffusion or first order regularisation terms for non-parametric image registration.

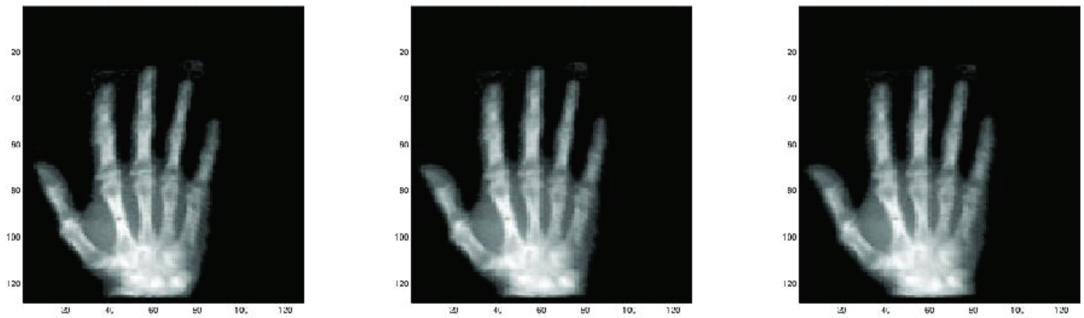

(a) M1B, $\varepsilon = 0.0524$ (b) M2B, $\varepsilon = 0.0378$ (c) M3B, $\varepsilon = 0.0284$

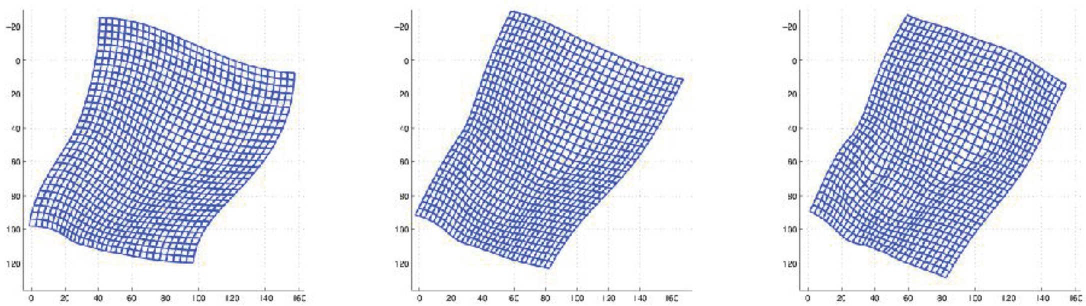

(d) $\gamma = 4, F = 0.4850$ (e) $\gamma = 1, F = 0.5457$ (f) $\gamma = 0.1, F = 0.3833$

FIGURE 3. Test 1: from left to right and top to bottom. Top row: (a) is the transformed template image using the linear curvature model for image registration method. (b) is the resulting transformed template image using the linear curvature and affine as a pre registration. (c) is the transformed template image using the decomposition model with affine and linear curvature models. The images on the bottom row are the corresponding deformations to the top row applied on regular grid. We can observe that the lowest value of ε is given by the decomposition model indicates higher similarity between the reference and the transformed template images.

The results for COFIR and CBTV are shown in Figure 4 (a) and (b) respectively. Only COFIR and M3B are able to provide the correct transformation where the smallest value of $\varepsilon = 0.0284$ is given by M3B in (c).

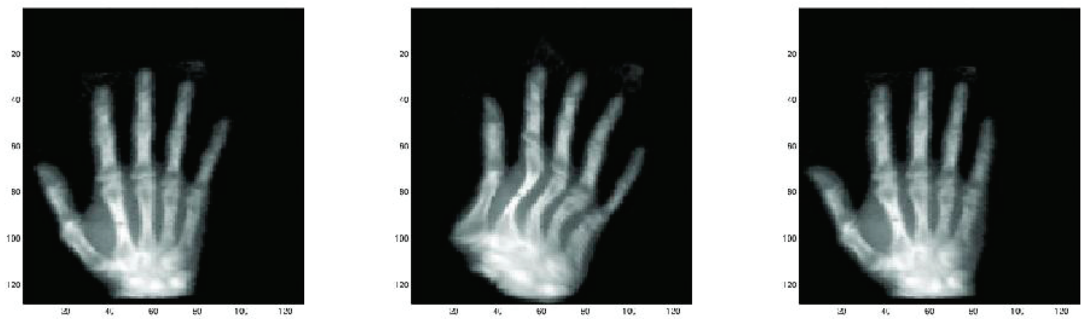

(a) $COFIR, \varepsilon = 0.0606$ (b) $CBTV, \varepsilon = 0.2208$ (c) M3B, $\varepsilon = 0.0284$

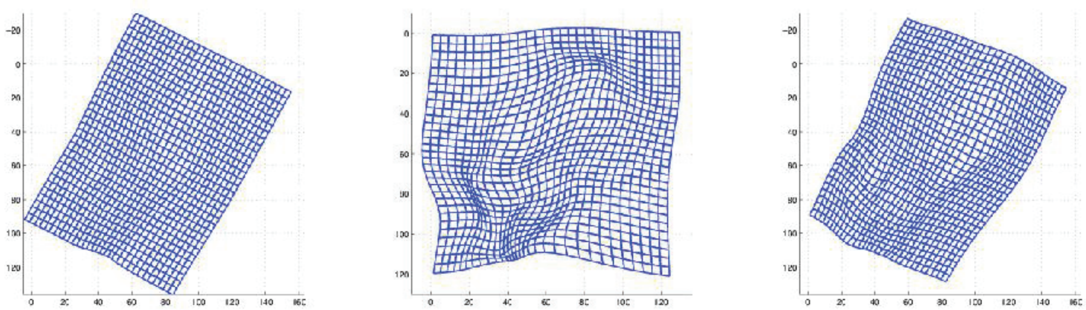

(d) $\gamma = 0.1, F = 0.5979$ (e) $\gamma = 0.05, F = 0.2038$ (f) $\gamma = 0.1, F = 0.3833$

FIGURE 4. Test 1: from left to right and top to bottom. Top row: (a) is the result using COFIR by Haber and Modersitzki [12, 13], (b) is using cubic B-spline and total variation model in Hu et al. [21] and (c) is the transformed template image using the decomposition model via Model B. The images on the bottom row are the corresponding deformations to the top row applied on the regular grid. COFIR and Model B are able to solve this particular problem but the best one is given by the decomposition Model B since the model has the smallest value of the dissimilarity measures indicating by ε .

CONCLUSION AND FUTURE WORK

We have presented a unifying framework for the decomposition models of parametric and non-parametric image registration. The models can be effectively solved using a Lagrangian method in multilevel implementation. Numerical experiments show that the models outperforms the single non-parametric models and the non-parametric models with affine as the pre-registration step. Out of the possible decomposition model that we already investigate, the model given by affine and linear curvature (Model B) turns to be the most effective and efficient model based on the numerical results obtained.

Future work will involve developing an efficient multigrid method to solve the model and automatic selection of regularisation parameters.

ACKNOWLEDGMENTS

The research and writing of this work was partially carried out under UPNM short term grants: UPNM/2016/GPJP/3/SG/3 and UPNM/2016/GPJP/3/SG/4.

REFERENCES

1. M. Holden, IEEE T. Med. Imaging **27,** 111–28 (2008).
2. J. A. Maintz and M. A. Viergever, Med. Image Anal. **2**, 1–36 (1998).
3. B. Zitov and J. Flusser, Image Vision Comput. **21**, 977–1000 (2003).
4. D. Rueckert and J. Schnabel, in Biomedical Image Processing (Springer, 2011), pp. 131–154.
5. J. Modersitzki, Numerical Methods for Image Registration (Oxford University Press, 2004).
6. J. Modersitzki, Flexible Algorithms for Image Registration (SIAM publications, 2009).
7. N. Chumchob and K. Chen, Int. J. Numer. Anal. Mod. **6**, 311–334 (2009).
8. D. Rueckert, L. I. Sonoda, C. Hayes, D. L. Hill, M. O. Leach, and D. J. Hawkes, IEEE T. Med. Imaging **18**,712–21 (1999).
9. J. P. Thirion, Med. Image Anal. **2**, 243–260 (1998).
10. C. Broit, "Optimal registration of deformed images," Ph.D. thesis, University of Pennsylvania 1981.
11. B. Fischer and J. Modersitzki, in Computational Science ICCS 2002 (Springer, 2002), pp. 202–206.
12. E. Haber and J. Modersitzki, "COFIR: coarse and fine image registration," in SIAM Real-Time PDE Constrained Optimization (SIAM, 2007), pp. 37–49.
13. J. Modersitzki and E. Haber, "Cofir: Coarse and fine image registration," Tech. Rep. (Emory University, 2004).
14. B. Fischer and J. Modersitzki, J. Math. Imaging Vis. **18**, 81–85 (2003).
15. N. Chumchob and K. Chen, Numerical Methods for Partial Diffrential Equations **28**, 1966–1995 (2012).
16. 16 N. Chumchob, K. Chen, and C. Brito-Loeza, Multiscale Model. Simul. **9**, 89–128 (2011).
17. M. Ibrahim, K. Chen, and C. Brito-Loeza, Journal of Geometry, Imaging and Computing **1**, 417–446 (2014).
18. S. Henn and K. Witsch, SIAM J. Sci. Comput. **23**, 1077–1093 (2001).
19. R. Bajcsy and S. Kovaˇciˇc, Comput. Vision Graph. **46**, 1–21 (1989).
20. J. C. Gee and R. K. Bajcsy, "Elastic matching: Continuum mechanical and probabilistic analysis," in Brain Wraping (Academic Press, 2000), pp. 193–198.
21. W. Hu, Y. Xie, L. Li, and W. Zhang, Neurocomputing **144**, 222–237 (2014).
22. A. Myronenko and S. Xubo, IEEE Transactions on Medical Imaging **29**, 1882–1891 (2010).
23. Z. Xie and G. E. Farin, IEEE T. Vis. Comput. Gr. **10**, 85–94 (2004).
24. U. Trottenberg and A. Schuller, Multigrid (Academic Press, 2001).